Geochemistry and petrogenesis of Tertiary mafic dykes from Taleghan, North Iran

Behnaz Hosseini[*1] , Ahmadreza Ahmadi[1]

1- Assistant professor, Department of Geology, Payame Noor University.

* Corresponding Author: Be.hosseini@gmail.com

Received: 13 May 2016 / Accepted:21 August 2016 / Published online: 25 December 2016

Abstract

In Taleghan, olivine basalt-basaltic andesite Dykes as part of Tertiary mamgmatic activities in central and western Alborz zone, intruded into both Karaj Formation and late Eocene-Oligocene volcanic rocks. These dykes have similar geochemical characteristic which suggest that they are originated from a common source. On the primitive mantle normalized spider diagram, the dykes are characterized by enrichment of LILEs and depletion of HFSEs. In general, these rocks show geochemical characteristics of volcanic rocks originated from partial melting of metasomatized lithospheric mantles in active continental margins. On the other hand, post collisional magmatism and anomalous thin continental crust beneath the Alborz zone confirm that extensional tectonic activities played a major role in this part of Iran. In this model, the subduction related magmas were produced by partial melting of a previously metasomatized lithospheric mantle source developed by percolation of fluid-melt released from subducted oceanic slab.

Keywords: Dyke; Geochemistry; Tertiary; Alborz; Taleghan, Iran.

1- Introduction

The bulk of the Cenozoic magmatism in Iran is focused in central (Urumieh-Dokhtar belt) and Northern (Alborz belt) Iran. A large amount of volcanism occurred in the Alborz during the Tertiary contemporary to same volcanic rocks in the Achara–Trialet belt of Georgia and the Pontides of northern Turkey (Kazmin *et al*., 1986). The Alborz Mountains of northern Iran with an average elevation of nearly 3000 m (Dehghani and Makris, 1984; Rodgers *et al*., 1997; Seber *et al*., 1997; Guest *et al*., 2007a) extend laterally 900 km around the south Caspian Sea and are located 200-500 km north of the Neo-Tethyan suture (Fig. 1). This polyorogenic mountain is a part of the Alpine-Himalayan active tectonic belt that was affected by the Eocimmerian and the Alpine orogenies. To the west and on its southern side, the Alborz is juxtaposed against the Urumieh-Dokhtar magmatic assemblage (UDMA), an magmatic arc complex related to the subduction of the Neo-Tethyan oceanic realm during late Mesozoic and Cenozoic time (Alavi. 1994). Hassanzadeh *et al* (2004) propose that the Alborz and The Urumieh-Dokhtar magmatic arc initiated as one continental marginal magmatic arc that was subsequently rifted apart. Alavi (1996) suggest a double subduction-zone model of Cretaceous-Paleogene magmatic belts of the Alborz Mountains and the Urumieh-Dokhtar. On the base of this model, the magmatic assemblage of the Alborz is a result of a Subduction of the Neo-Tethyan marginal sea (behind the Urumieh-Dokhtar) beneath the Alborz continental margin from late Cretaceous to Early Eocene. Also he believes that the juxtaposition of the southwestern part of the Alborz and the Urumieh-Dokhtar is a result of the collision between the magmatic assemblages of the Urumieh-Dokhtar and Alborz. The Alborz belt consists mainly of sedimentary strata in the late Precambrian to the Eocene and volcanic rocks in the Tertiary. These are

intruded by Paleozoic to Pleistocene plutons and dykes.

In western and central Alborz, upper Cretaceous to Recent magmatic rocks both submarine and subaerial, mainly of calcalkaline to shoshonitic types (Dostal and Zebri, 1978; Asiabanha, 1992) form a distinct curvilinear belt. In the south-central Alborz, the Karaj Formation unconformably overlies the older deformed sequences (guest 2006). The Karaj Formation consists mostly of submarine calcalkaline, acidic and andesitic tuffs and shales (Dedual, 1967; Annells *et al*., 1975; Berberian and Berberian, 1981) deposited in a deep marine basin (Berberian, 1983; Hassanzadeh *et al*., 2002; Guest *et al*., 2006). Fossil assemblages identified from calcareous rocks within this sequence indicate a stratigraphic range of Middle Eocene (Lutetian) to Lower Oligocene (Stalder, 1971). The Karaj Formation is unconformably overlain by subaerial, basic to acidic volcanic rocks of earliest Oligocene age. The magmatic activity of the Alborz is likely to be related to the subduction of Arabia–Eurasia collision, but the details remain poorly understood (Allen, 2003).

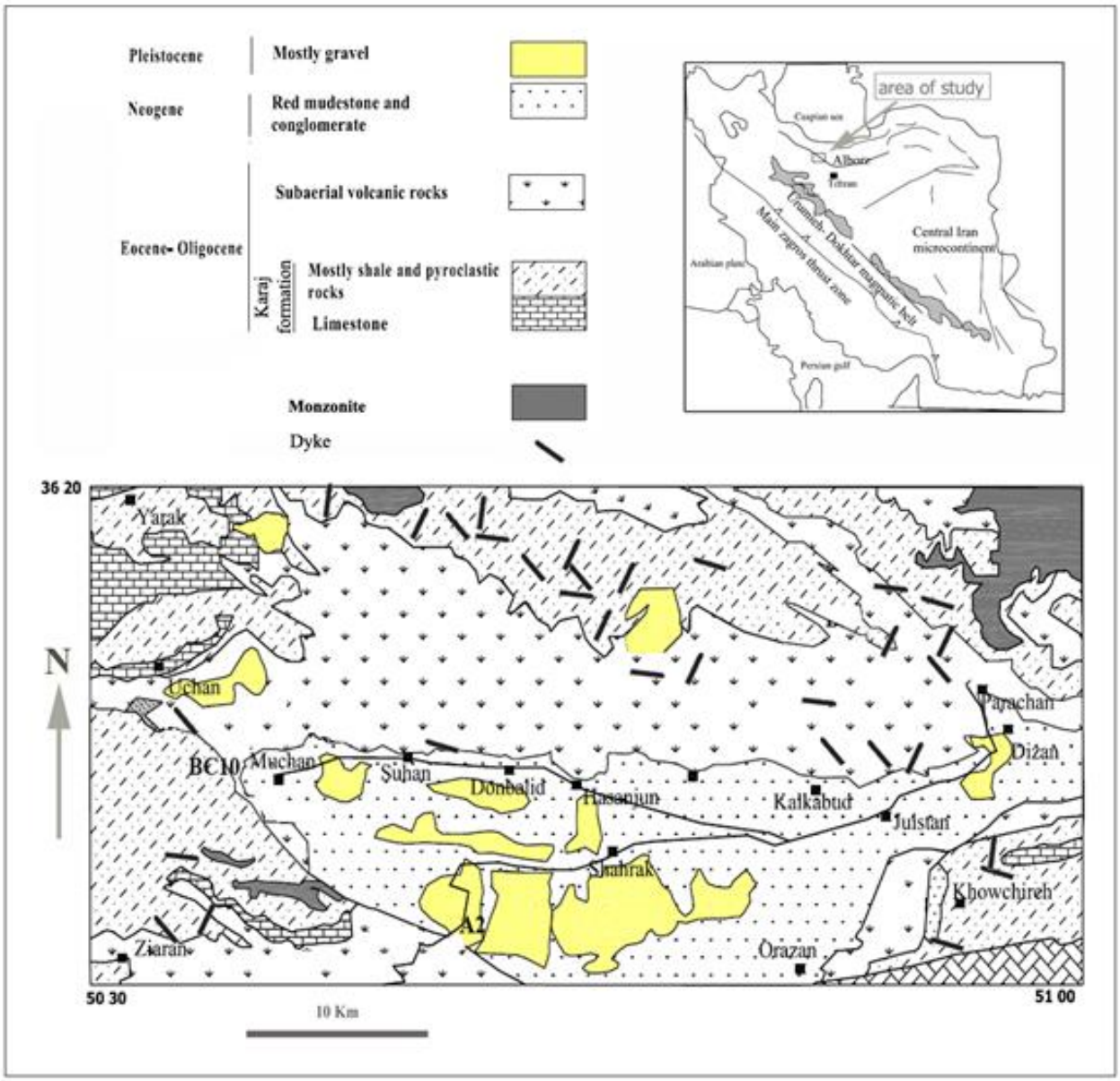

Figure 1) Simplified geological map of Iran and geological map of the Taleghan area (modified from Annells et al., 1977).

In this study, the petrology and geochemistry of mafic dykes in Taleghan are discussed. The aim of this study is to propose an origin for the magmas and also the tectonomagmatic setting in which magmatism occurred. The study area covers part of magmatic rocks cropped out from central to western Alborz.

2- Geological setting of study area

The Taleghan region located 80 km northwest of Tehran in north of Iran, is situated in the south side of Central Alborz zone (Fig. 1). This region has a late Precambrian basement (Kahar Formation) covered by Cambrian to Eocene sedimentary layers with a thickness reaching 6-7 km (Annells *et al*., 1975). The Tertiary sequence (with a thickness nearly 6000 m) overlaps with marked unconformity on to older formations however the Palaeocene and Lower Eocene rocks are not present in the area. These rocks show great lateral variations in thickness due variously to the highly irregular relief of the Pre-Paleogene surface and the continuation of crustal movement from late Cretaceous time through the Eocene (Annells *et al*., 1975). This sequence comprises two major parts (Fig. 1). The lower part (Karaj Formation) consists of up to 3000 m of mainly green- grey tuffs, of acid composition, with intercalated dacitic sheets up to 150 m thick. In some areas the Karaj Formation also includes dark-grey tuffaceous mudstones, probably derived from extensive crops of Cretaceous lava, and nummulitic limestone.

Figure 2) Field features of mafic dikes. a) A dyke with 2 meters width intruded in sedimentary units of the Karaj Formation in north of Ziaran village; b) A dyke with approximately 0.5 meter width intruded the Eocene volcanic units in north of Kalkabud village.

The upper part (subaerial volcanic rocks) consists of up to 2500 m of mainly basic lava flows of probable upper Eocene to Oligocene age (Annells *et al*., 1975). Transition between the first stage (Karaj formation) and the second stage (Subaerial volcanism) is sharp over most of area, but is sometimes gradational and lavas and tuffs are interbedded in equal proportion over 100 m transitional zone (Stalder, 1971). Zones of vesicles occur in the lower and upper part of sequence. Subaerial volcanic rocks are subdivided into two distinct phases (Ahmadi and Ghorbani, 2010). The first phase demonstrate the geochemical characteristics of active continental margin volcanics derived from an enriched lithospheric mantle while second phase show the geochemical characteristics of intraplate volcanics derived from asthenospheric plumes (Ahmadi and Ghorbani, 2010). Numerous mafic dykes cut the Karaj Formation (Fig. 2a) and Tertiary volcanic rocks (Fig. 2b). The dykes vary in thickness from less than 1 meter to more than several meters. These dykes are probably feeder dykes

for Tertiary volcanic units in the study area. The subaerial volcanic rocks are unconformably overlain by a sequence of over 2000 m of Neogene red beds comprise conglomerates, breccias and fine clastic sediments.

Table. 1) Major oxides and trace element contents of representative samples.

Sample	TD1	TD2	TD3	TD4	TD5	TD6	TD7
(wt.%)							
SiO_2	46.43	52.16	48.65	53.86	46.36	50.17	54.53
Al_2O_3	15.68	20.41	17.45	19.26	15.27	18.15	19.57
Fe_2O_3	11.44	8.31	9.12	8.16	11.57	11.23	7.11
MgO	8.27	3.77	5.28	3.67	8.13	4.34	2.53
CaO	10.79	6.62	11.38	7.44	11.52	7.86	6.14
Na_2O	3.25	3.93	5.16	3.1	2.7	3.28	5.89
K_2O	1.14	1.16	0.64	2.1	0.84	1.96	1.16
TiO_2	1.24	0.84	1.05	0.86	1.16	0.92	1.07
P_2O_5	0.72	0.87	0.62	0.46	0.63	0.95	0.38
MnO	0.2	0.14	0.22	0.25	0.2	0.26	0.3
(ppm)							
Ba	757	1632	1084	1773	938.5	1562	1482
Ce	40.23	99.43	58.63	86.34	48.43	87.47	76.06
Dy	4.23	5.24	4.96	5.63	4.32	5.05	5.97
Er	2.27	3.55	2.72	3.42	2.34	2.95	3.73
Eu	1.46	2.15	2.07	2.43	1.86	2.36	2.81
Gd	3.75	6.35	4.95	6.58	4.57	6.26	6.86
Hf	1.37	3.75	2.83	4.15	2.64	3.53	4.58
Ho	0.88	1.1	0.81	1.18	0.93	0.94	1.32
La	20.48	40.63	34.84	48.47	25.4	36.93	53.96
Lu	0.25	0.43	0.38	0.46	0.31	0.4	0.51
Nb	6.27	12.16	10.87	13.25	9.72	11.33	15.57
Nd	20.63	40.62	33.59	43.63	29.52	42.56	50.12
Pb	10.43	25.79	18.27	26.82	15.83	27.43	27.86
Pr	5.24	10.66	7.55	11.42	6.84	9.56	12.05
Rb	84.76	85.48	99.76	111.9	73.95	125.54	137.74
Sm	4.67	7.24	5.96	7.95	5.37	7.92	8.52
Sr	673	1153.7	1086.8	1263.3	974.5	1263.7	1386.4
Ta	1.14	1.27	1.23	1.21	1.05	1.17	1.27
Tb	0.664	0.92	0.86	0.868	0.74	0.75	0.96
Th	5.24	11.24	9.54	11.65	8.97	11.72	13.16
Tm	0.33	0.46	0.41	0.42	0.36	0.39	0.5
U	1.74	3.41	2.65	3.62	2.15	3.1	4.26
Y	19.42	28.91	27.54	29.95	23.63	28.38	32.73
Yb	1.53	2.16	2.22	2.36	1.87	2.06	2.94
Zr	56.34	168.8	94.52	174.32	84.32	108.54	158.8

3- Petrography

In hand specimen, these rocks are massive with dark grey to black color and carry abundant dark pyroxene. Petrographic studies show that the rocks are porphyritic (Fig 3a and b) with phenocrysts of rectangular plagioclase, up to 5 mm long, subhedral to euhedral clinopyroxene, up to 5 mm long, subhedral olivine, up to 3 mm long and magnetite set in a holocrystalline to hyaline matrix. Total phenocryst contents vary from 30 to 60% (by volume). Partial to complete replacement of Olivine by iddingsite or green serpentine is common in these rocks. Twinning of clinopyroxene and Plagioclase crystals is common. Some samples show glomerophyric clots of plagioclase probably as a consequence of plagioclase accumulation. In more evolved rocks, k-feldespar occurs as rime around plagioclase phenocrysts or as minor

crystals in matrix. The groundmass is composed of plagioclase, clinopyroxene, and magnetite and in more evolved rocks K-feldespar. Apatite is present as accessory mineral in groundmass.

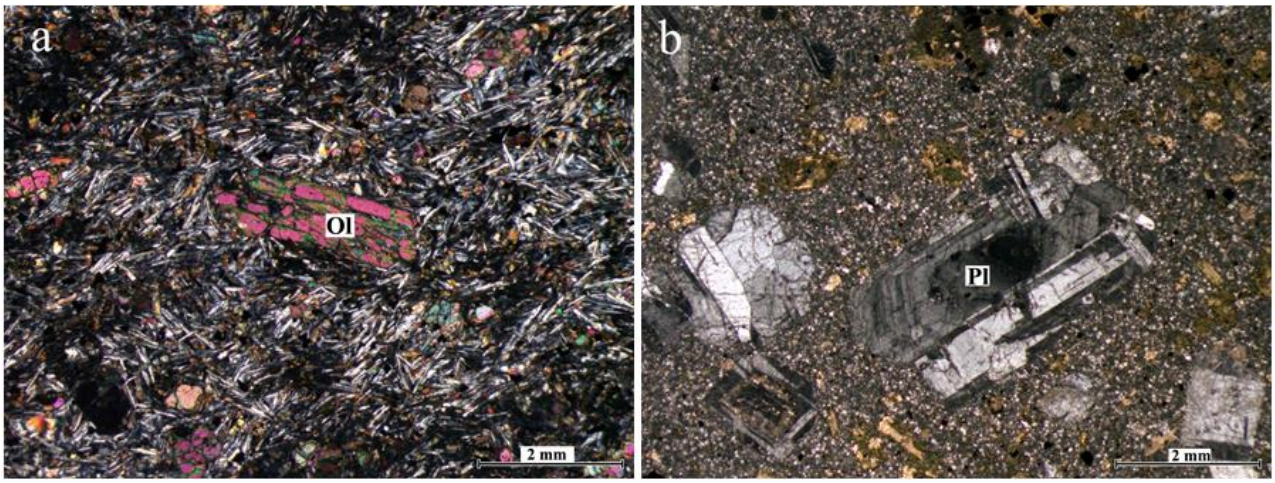

Figure 3) Microphotographs of representative samples (crossed polarized light). (a) Olivine basalt with microlithic groundmass; (b) large plagioclase pheonocrysts in a basaltic andesite. Ol: Olivine, Pl: Plagioclase.

4- Materials and methods

4.1- Analytical methods

Seven representative samples from the mafic dykes were chosen for major and trace element analysis. Major and trace elements were determined by ICP-Ms method (LF-200 collection) at the Acme analytical laboratories, Canada.

4.2- Major and trace elements chemistry

Whole-rock major, trace and rare earth elements analyses of 7 representative samples are given in Table 1. Samples span a range of 46.36-54.53 wt. % SiO_2 with MgO of 2.53-8.27 wt. %. The abundance of TiO_2 varies between 0.84 and 1.24 wt. %. The samples have elevated contents of Al_2O_3 (15.27-20.41 wt %). Additionally, all of them have a K_2O/Na_2O ratio < 1.

In the total alkali-silica diagram (Le Maitre, 1989), the samples fall in the fields of basalt, trachy basalt and basaltic trachy andesite (Fig. 4a). The division between the alkaline and subalkaline field defined by Irvine and Baragar (1971) has also been plotted onto this diagram (dashed line). All the samples fall in the alkaline field or near the dividing line (Fig. 4a). However, in The Zr/TiO_2 versus Nb/Y diagram of Winchester and Floyd (1977), the samples plot in the sub-alkaline basalt to andesite field (Fig. 4b). Also we classify these rocks using the K_2O vs. SiO_2 diagram (Peccerillo and Taylor, 1976) (Fig. 4c). This diagram suggests calc-alkaline to high- K calc- alkaline nature for these rocks.

MgO is used as an index of differentiation to qualitatively identify processes that may be responsible for chemical variations in the mafic rocks. Fig. 5 shows the major elements plotted against MgO for Taleghan dykes. These diagrams show that in general the samples follow coherent patterns. In summary, The systematic decrease of SiO_2, Al_2O_3, Na_2O + K_2O and increase of CaO, FeO*, TiO_2, CaO/Na_2O and CaO/Al_2O_3 with decreasing MgO contents indicate that fractional crystallization of ferromagnesian minerals such as olivine, clinopyroxene and Ti-bearing opaques may have played an important role in the magmatic evolution. CPX fractionation is supported by the strong correlation of CaO/Na_2O ratios with MgO content. The CaO/Na_2O ratio is virtually independent of pressure of melting (Herzberg and Zhang, 1996) and of olivine fractionation, but is very sensitive to clinopyroxene fractionation.

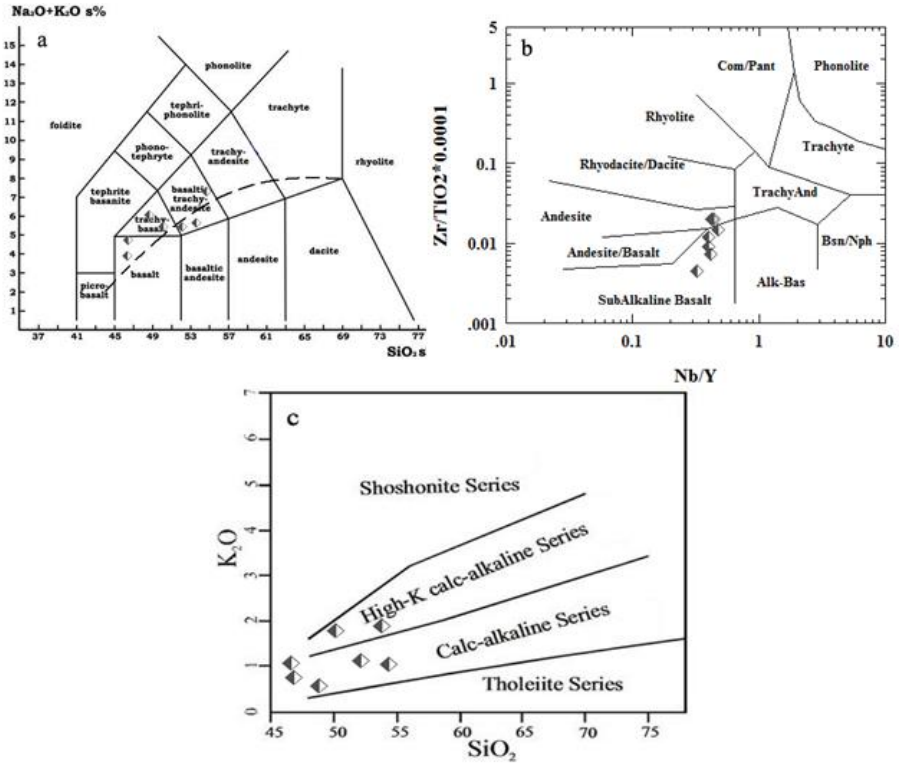

Figure 4a) SiO_2 versus K_2O+Na_2O (after Le Maitre, 1989); b) Nb/Y versus SiO_2 (after Winchester and Floyd, 1977); c) K_2O versus SiO_2 (after Peccerillo and Taylor, 1976).

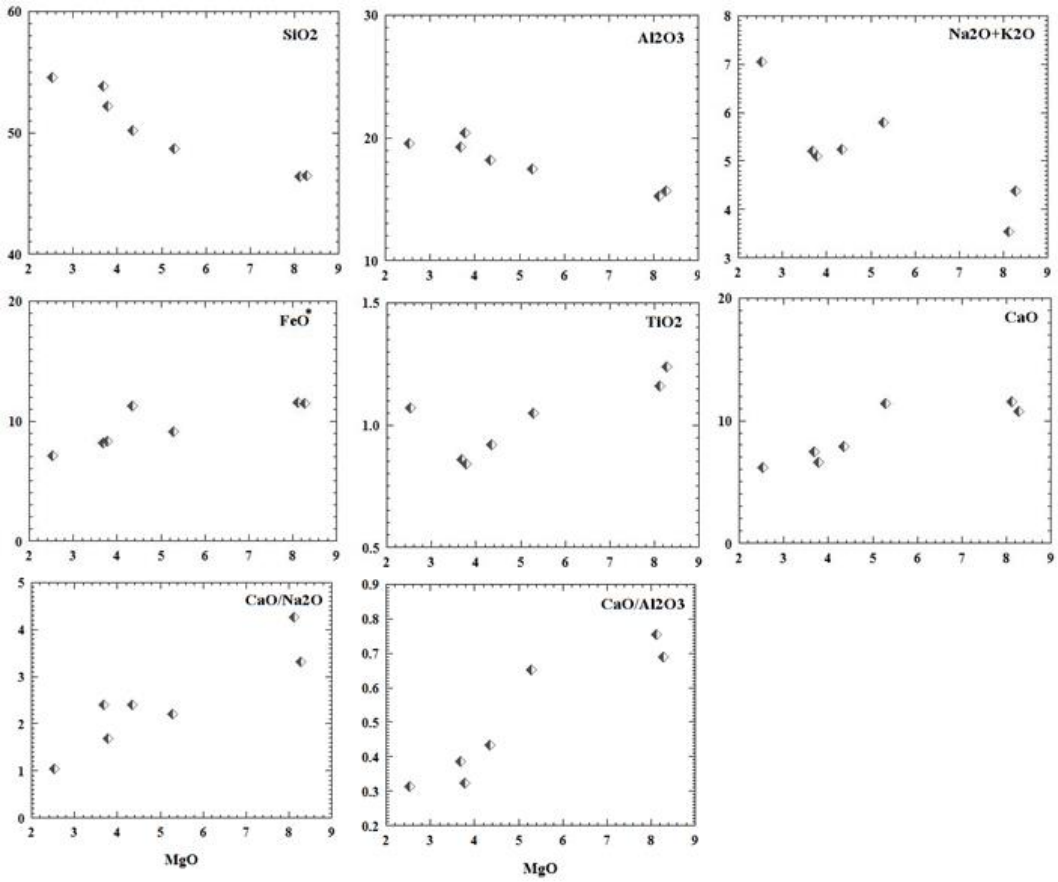

Figure 5) Variation diagrams of major oxides vs. MgO.

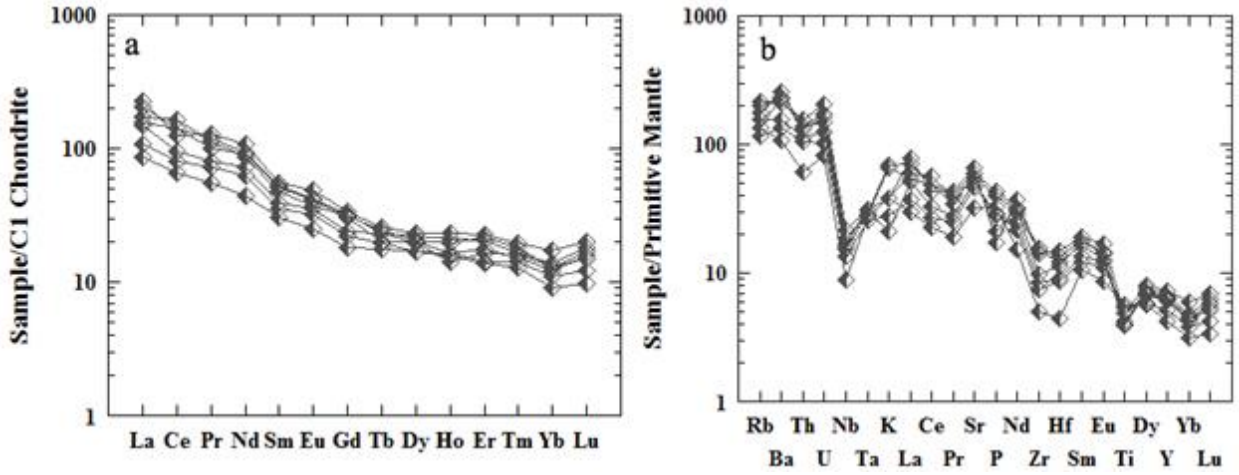

Figure 6a) Chondrite-normalized rare-earth element patterns (The normalizing values are from Sun and McDonough, 1989); b) Primitive mantle-normalized trace element diagrams (The normalizing values are from Sun and McDonough, 1989).

Increasing Na_2O and K_2O trends with decreasing MgO is typical because none of early formed phases contain those elements.

The chondrite-normalized rare earth elements (REE) patterns for these mafic rocks are quite similar and (Fig. 6a) reveal enrichment of light rare earth elements (LREE) over heavy rare earth elements (HREE). REE concentrations increase, in general, with increasing silica, creating a moderate enrichment in M- to HREEs and a more profound enrichment in LREEs. The $(Gd/Yb)_{Cn}$ ratio ranges between 2.2 to 3.7 indicating slight differentiation between MREEs to HREEs. The absence of Eu anomalies implies that while feldspar phenocryts are abundant in the rocks, their removal during fractionation was not significant.

Primitive mantle-normalised multi element patterns are given in Fig. 6b. The patterns exhibit significant enrichment of LILE (K, Rb, Ba and U) and Th over REEs with a negative anomaly at HFSE (Ta, Nb, Zr and Ti) relative to neighbor elements. The patterns of these rocks are typical of subduction-related mafic rocks or continental intraplate basalts that have been significantly contaminated or derived from a lithospheric mantle modified by an ancient subduction process.

5- Discussion

In order to determine the geotectonic environment, trace-element contents of the samples are plotted on the Hf-Th-Nb diagram (Wood, 1980). All the samples populate the subduction related field (Fig. 7a).

The source characteristics of these rocks can be determined by using some trace element ratios (e.g., Ce/Pb, Sm/Yb, Ce/Sm, Nb/Th) which are relatively insensitive to degree of partial melting and secondary mobilization (Pearce, 1982; Hofmann, 1988; Sun and McDonough, 1989). The samples plot in the arc volcanic subfield in the Ce/Pb vs. Ce diagram (Fig. 7b).

The nature of fluid or flows that affected mantle metasomatism is evidenced in the Rb/Y vs. Nb/Y diagram showing that the rocks plot next to the trend of subduction zone enrichment or crustal contamination (Fig. 8a).

The igneous rocks show significant negative Nb, Ta, Ti, Zr and Hf anomalies and enrichment in LILs and LREEs (Fig. 6b). These characteristics however indicate either an arc signature or crustal contamination in the evolution of magmas (Pearce, 1982; Wilson, 1989). In other hand it is important to know that geochemical features which are relevant to the origin of these rocks are related to a significant crustal contamination or to a source enriched in

LREE and depleted in HREE and HFSE relative to primitive mantle. Continental crust has been characterized by highly fractionated and enriched LREE, flat HREE, a positive Pb but negative anomalies at Nb–Ta (Taylor and McLennan, 1985). As the Taleghan magmas were erupted through continental crust, crustal contamination is a possibility. However, the high Ti/Y and low Rb/Ba of these rocks are features not generally ascribed to the continental crust and these rocks do not lie on simple mixing lines between crust and asthenospheric magmas (Fig. 8b).

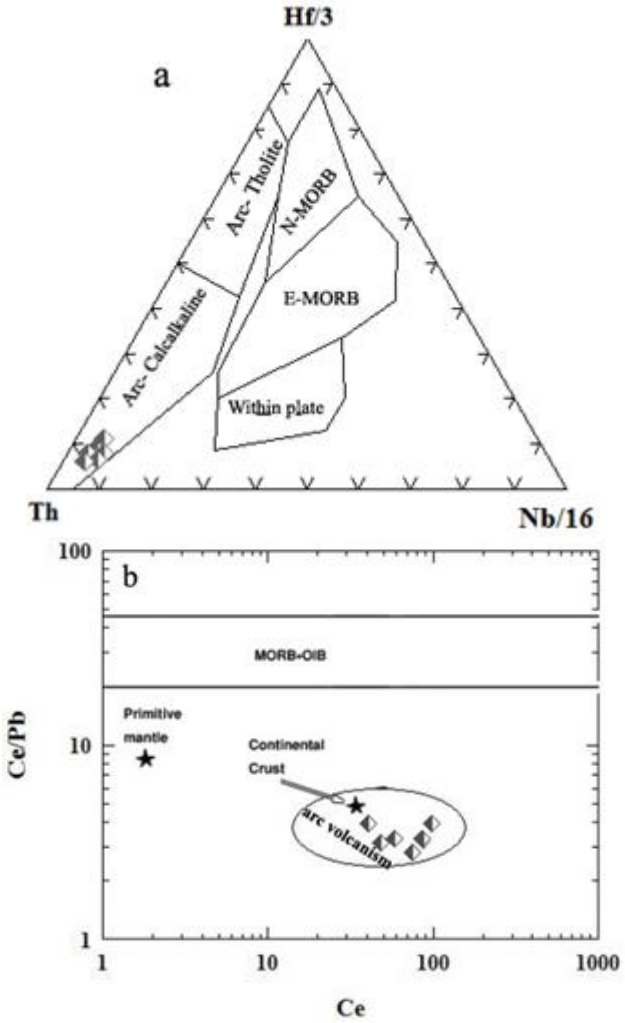

Figure 7a) Hf-Th-Nb diagram (Wood, 1980); b) Ce/Pb versus Ce diagram (The data are obtained from Hofmann et al., 1986).

This implies that magma was derived from a mantle source that had been previously enriched by a subduction component (in which Th is more soluble than Ta and Yb). On the base of this, High field strenght elements (e.g., Ta, Nb, Ti) are retained in the subducting slab, whereas low field strenght elements (e.g., Rb, Sr, K, Ba, U) are easily transported to the overlying zone of mantle melting (Pearce, 1982). The low Rb/Ba (0.05-0.1) and Rb/Sr (0.07-0.12) ratios accompanied by high Ba and Sr contents suggest enrichment of mantle peridotite by silicate melts rather than by hydrous fluids (Miller *et al*., 1999).

The Ba/Nb ratios of the samples range between 95.2 and 137.8. Ba/Nb ratio of the active continental margin magmatism is greater than 28 (Fitton *et al*., 1987). Thus, these high Ba/Nb values are characteristics of active continental margin related magmatism.

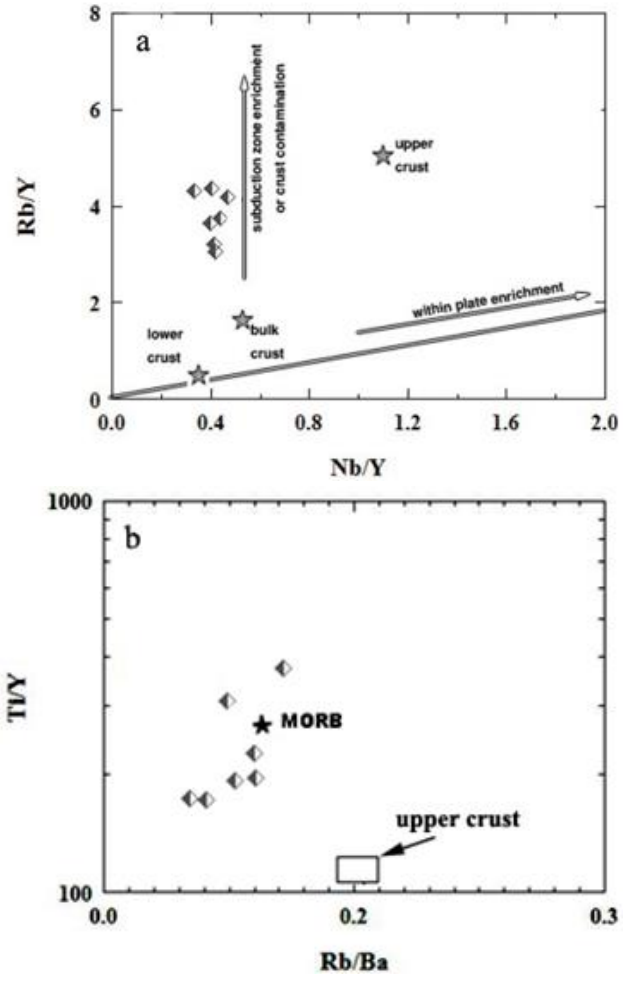

Figure 8a) Plot of Rb/Y versus Nb/Y (after Termel et al., 1998): Samples plot along subduction zone enrichment & crustal contamination trend; b) Ti/Y versus Rb/Ba (Turner et al., 1996): The studied samples do not distinctively plot in either mantle derived magmas or upper crustal magmas fields.

Lithospheric mantle has high and variable degree of La/Nb, which is generally higher than 1, whereas asthenospheric magma source has a low, well-defined ratio of La/Nb (0.7) (DePaolo and Daley, 2000). The La/Nb ratios of these rocks vary from 2.6 to 3.6. Combination of this information with trace-element patterns (Fig. 6b) indicates that the mantle sources in the genesis of these rocks were lithospheric mantle.

6- Conclusions

Mafic dykes in Taleghan show typical geochemical characteristics of subduction related magmatic rocks along active continental margins. Accordingly, these dykes resemble volcanic rocks of episode 1 in Taleghan, and can be considered as feeder dykes for the volcanic rocks. The crust of the Alborz mountain range is relatively thin (less than 35 km) in relation with its high elevation, which points to the role of a period of tensional tectonic regimes after continental collision. The Eocene-Oligocene volcanic rocks probably represent volcanism occurred during the tensional regimes which led to a reduction in crust thickness. Lithospheric mantle previously metasomatized by aqueous fluids-melts released from the Neotethyan oceanic crust, underwent partial melting due to a post-collisional crustal extension to generate magmas with typical geochemical signatures of subduction-related magmas.

References

Ahmadi, A.R., Ghorbani, M.R., 2010. The origin and tectonomagmatic setting of Taleghan Tertiary volcanic rocks. Iranian Journal of Geology: 4, 83–99 (in Farsi).

Alavi, M., 1994. Tectonics of the Zagros orogenic belt of Iran: New data and interpretations. Tectonophysics: 229, 211–238.

Alavi, M., 1996. Tectonostratigraphic synthesis and structural style of the Alborz Mountain System in Iran. Journal of Geodynamics: 21/1, 1e33.

Allen, M., Ghassemi, M. R., Shahrabi, M., Qorashi, M., 2003. Accommodation of late Cenozoic oblique shortening in the Alborz range, northern Iran. Journal of Structural Geology: 25, 659–672.

Annells, R. N., Arthurton, R. S., Bazley, R. A., Davies, R. G. 1975. Qazvin and Rasht; 1:250,000 scale geological quadrangle map. Geological Survey of Iran.

Annells, R. S., Arthurton, R. S., Bazley, R. A. B., Davies, R. G., Hamedi, M. A. R., Rahimzadeh, F. 1977. The 1:100,000 geological map of Shakran, sheet no. 6162, Tehran, Geological Survey of Iran.

Asiabanha A. 1992. Petrology and geochemistry of the volcanic rocks of the Molla-Ali area, northwest of Ghazvin. MSc. Thesis, Department of Geology, University of Tehran, Tehran, pp. 152 (in Farsi).

Berberian, F., Berberian, M., 1981. Tectono-plutonic episodes in Iran. In: Delany, F.M. (Ed.), Zagros–Hindu Kush–Himalaya Geodynamic Evolution. Geodynamics Series. American Geophysical Union, Washington, D.C., pp. 5–32.

Berberian, M. 1983. The southern Caspian: A compressional depression floored by a trapped, modified oceanic crust. Canadian Journal of Earth Science 20, 163–183.

Dedual, E. 1967. Zur Geologie des mittleren und unteren Karaj-Tales, Zentral-Elburz (Iran): Mitteilungen aus dem Geologischen Institut der Eidgenossischen Technischen Hochschule und der Universität Zürich, Neue Folge, v. 76, p. 123.

Dehghani, G. A., Makris, J. 1984. The gravity field and crustal structure of Iran. Neues Jahrbuch für Geologie und Paläontologie: 168, 215– 229.

DePaolo, D.J., Daley, E.E., 2000. Neodymium isotopes in basalts of the southwest basin and range and lithospheric thinning during continental extension. Chemical Geology: 169, 157–185.

Dostal, J., Zebri, M. 1978 Geochemistry of Savalan volcano (Northwestern Iran): Chemical Geology: 22, 31–42.

Fitton, J. G. 1987. The Cameroon line, West Africa: a comparison between oceanic and continental alkaline volcanism. In: Fitton, J.G. Upton, B.G.J. (Eds.), Alkaline Igneous Rocks. Geological Society of London, Special Publication: 30, 273–291.

Guest, B., Guest, A., Axen, G. 2007a. Late Tertiary tectonic evolution of northern Iran: A case for simple crustal folding. Global and Planetary Change: 58, 435–453.

Guest, B., Stockli, D. F., Grove, M., Axen, G. J., Lam, P. S. Hassanzadeh, J. 2006b. Thermal histories from the central Alborz Mountains, northern Iran: implications for the spatial and temporal distribution of deformation in northern Iran. Geological Society of America Bulletin: 118, 1507–1521.

Hassanzadeh, J., Ghazi, A. M., Axen, G., Guest, B. 2002. Oligomiocene mafic-alkaline magmatism in north and northwest of Iran: evidence for the separation of the Alborz from the Urumieh-Dokhtar magmatic arc. Geological Society of America Conference, Denver, Colorado, p. 331.

Hassanzadeh, J., Axen, G., Guest, B., Stockli, D. F., Ghazi, A. M. 2004. The Alborz and NW Urumieh-Dokhtar magmatic belts, Iran: rifted parts of a single ancestral arc. Geological Society of America National Meeting. Geological Society of America Conference, Denver, Colorado, p. 434.

Herzberg, C., Zhang, J. 1996. Melting experiments on anhydrous peridotite KLB-1: compositions of magmas in the upper mantle and transition zone. Journal of Geophysical Research: 101, 8271–8295.

Hofmann, A. W., Jochum, K. P., Seufert, M. 1986. Nb and Pb in oceanic basalts: new constraints on mantle evolution. Earth and Planetary Science Letters: 79, 33–45.

Hofmann, A. W. 1988. Chemical differentiation of the Earth: the relationship between mantle, continental crust, and the oceanic crust. Earth and Planetary Science Letters: 90, 297–314.

Irvine, T. N., Baragar, W. R. A. 1971. A guide to the chemical classification of the common volcanic rocks. Canandian Journal of Earth Sciences: 8, 523–548.

Kazmin, V. G., Sborthshikov, I. M., Ricou, L. E., Zonenshain, L. P., Boulin, J., Knipper, A. L. 1986. Volcanic belts as markers of the Mesozoic- Cenozoic active margin of Eurasia. Tectonophysics: 123, 123–152.

Le Maitre, R. W. 1989. A Classification of Igneous Rocks and Glossary of Terms (Recommendations of the International Union of Geological Sciences Sub-commission on the Systematics of Igneous Rocks). Blackwell, Oxford 193pp.

Miller, C., Schuster, R., Klotzli, U., Frank, W., Purtscheller, F. 1999. Post-collisional potassic and ultrapotassic magmatism in SW Tibet: geochemical and Sr-Nd-Pb-O isotopic constraints for mantle source characteristics and petrogenesis. Journal of Petrology: 40, 1399–1424.

Peccerillo, A., Taylor, S. R. 1976. Geochemistry of Eocene calcalkaline volcanic rocks from the Kastamonu area, northern Turkey. Contributions to Mineralogy and Petrology: 58, 63–81.

Pearce, J. A. 1982. Trace element characteristics of lavas from destructive plate boundaries. In: Thorpe, R.S. Ed., Andesites: Orogenic Andesites and Related Rocks. Wiley, New York, pp. 525–548.

Rodgers, A. J., Ni, J. F., Hearn, T. M. 1997. Propagation characteristics of short-period Sn and Lg in the Middle East. Bulletin of the Seismological Society of America: 87, 396–413.

Seber, D., Vallve, M., Sandvol, E., Steer, D., Barazangi, M. 1997. Middle East tectonics: applications of geographic information systems (GIS). GSA Today: 7, 1–5.

Stalder, P. 1971. Magmutisems tertiarie. Et subrecent entre Taleghan *et al*amout, Elbourz central (Iran). Bulletin Suisse de Minéralogie et Pétrographie: 51, 139PP.

Sun, S. S., McDonough, W. F. 1989. Chemical and isotopic systematic of oceanic basalts: implications for mantle composition and processes. In: Saunders, A.D., Norry, M.J. (Eds.), Magmatism in the Ocean Basins. Geological Society of London Special Publication: 42, 313–345.

Taylor, St. R., McLennan, S. M. 1985. The Continental Crust: its Composition and Evolution: 21, 85–86.

Termel, A., Gtlndogdu, M. N., Gourgaud, A., 1998. Petrological and geochemical characteristics of Cenozoic high K calc-alkaline volcanism in Konya, Central Anatolia, Turkey. Journal of Volcanology and Geothermal Research: 85, 327–354.

Turner, S., Arnaud, N., Liu, J., Rogers, N., Hawkesworth, C., Harris, N., Kelly, S., van Calsteren, P., Deng, W. 1996. Post-collision, shoshonitic volcanism on the Tibetan Plateau: implications for convective thinning of the lithosphere and the source of ocean island basalts. Journal of Petrology: 27, 45–71.

Wilson, M. 1989. Igneous Petrogenesis. Chapmann and Hall, London, 466PP.

Winchester, J. A., Floyd, P. A. 1977. Geochemical discrimination of different product using immobile elements. Chemical Geology: 20, 325–343.

Wood D. A. 1980. The application of a Th-Hf-Ta diagram to problems of tectonomagmatic classification and to establishing the nature of crustal contamination of basaltic lavas of the British Tertiary volcanic province. Earth and Planetary Sciences Letters: 42, 77–97.